Microwave Studies of Billiard Green Functions and Propagators

J. Stein, H.-J. Stöckmann, and U. Stoffregen
Fachbereich Physik, Universität Marburg, D-35032 Marburg, Germany
(Received 15 November 1995)

In a microwave transmission measurement the Green function $G(r, r', k)$ of a stadium billiard was determined as a function of r' and k for fixed r. From this billiard wave functions were obtained including the sign, which was not available earlier. The propagator $K(r, r', t)$ was obtained by Fourier transform of $G(r, r', k)$. It is shown that $K(r, r', t)$ supplies a very suggestive picture of pulse propagation including pulse reconstruction by focusing effects. This can be considered as an experimental verification of a work of Tomsovic and Heller, who found that semiclassical dynamics can account for the quantum mechanical behavior of billiards over surprisingly long times.

PACS numbers: 05.45.+b

Irregularly shaped billiards are favorite models to study the quantum mechanical properties of classically chaotic systems. In the last five years microwave analog experiments have become a well-established alternative to theoretical studies [1–4]. The experiments use the fact that the time-independent Schrödinger equation and the Helmholtz equation are equivalent. For quasi-two-dimensional billiards even the boundary conditions for the electromagnetic and the quantum mechanical systems are identical. In the first experiments eigenfrequencies of stadium-shaped microwave resonators were determined [1,2], but soon the method was extended to the study of eigenfunctions. There are two slightly different techniques to achieve this. Sridhar used the fact that the eigenfrequencies are shifted proportional to E^2 if a metallic bead is moved through the resonator [3]. Alternatively, E^2 can be obtained from the depth of the resonance as a function of the antenna position [4].

All experiments mentioned are incomplete insofar as they determine only eigenfrequencies ν_n and the absolute square of the wave function $|\psi_n(r)|^2$ as a function of position. To get the complete quantum mechanical information on the system, the billiard Green function

$$G(r, r', k) = \sum_n \frac{\psi_n(r)\psi_n(r')}{k_n^2 - k^2} \tag{1}$$

is required. k_n is the wave number of the nth eigenfrequency. The Green function obeys the differential equation

$$(\Delta + k^2)G(r, r', k) = -\delta(r - r'). \tag{2}$$

In this Letter we report on the first experiment in billiards where both the amplitude *and* phase of microwave reflection and transmission coefficients have been determined. From these quantities the complete Green function is easily obtained, as will be shown below. This allows a number of promising applications especially in the field of mesoscopic systems (universal conductance fluctuations, weak localization, etc.) [5]. From the Fourier transform of the Green function the propagator

$$K(r, r', t) = \sum_n \psi_n(r)\psi_n(r')e^{-i\omega_n t} \tag{3}$$

is obtained (with $\omega_n = 2\pi\nu_n$). In the semiclassical approximation it can be expanded into a sum over classical trajectories connecting points r and r' [6,7]. The propagator in a stadium was studied by Tomsovic and Heller [8], who found a correspondence between classical and semiclassical dynamics over times by far increasing the so-called log time $t = O(\ln(\hbar^{-1}))$. The exponential proliferation of the number of classical orbits limited the calculation of the classical trajectories to lengths corresponding to at most six horizontal traversals through the stadium. Here the experiment may provide an alternative. It should even be possible (though it was not yet done) to identify the contributions of different trajectories to the propagator by replacing parts of the walls by absorbing material thus suppressing all paths touching these regions.

To study billiard properties experimentally one has to install one or more antennas allowing for the excitation of microwaves. These antennas, on the other hand, unavoidably disturb and change the system properties. To describe reflection and transmission properties between different antennas the S matrix is very useful. It is defined by

$$b = Sa, \tag{4}$$

where a is the vector of amplitudes of the waves entering through the different channels and b is the amplitude vector of the outgoing waves. To establish a relation between the S matrix and the Green function, we can rely on results which have been derived in nuclear physics many years ago (see, e.g., Ref. [9]). To be self-contained the derivation is repeated here for the billiard case. With $\psi(r, k)$ as the wave function within the billiard if waves with wave number k are fed in through one or more open channels. $\psi(r, k)$ obeys the Helmholtz equation

$$(\Delta + k^2)\psi = 0. \tag{5}$$

Close to the position of the ith antenna ψ can be written as the superposition of an incoming and an outgoing wave,

$$\psi(r, k) = a_i \frac{H_0^{(1)}(k|r - r_i|)}{H_0^{(1)}(kR)} - b_i \frac{H_0^{(2)}(k|r - r_i|)}{H_0^{(2)}(kR)} \tag{6}$$

0031-9007/95/75(1)/53(4)$06.00

(assuming circular antennas with radius R). $H_0^{(1)}$ and $H_0^{(2)}$ are Hankel functions. From Eq. (6) one gets for ψ and its normal derivative on the surface S_i of the coupling wire

$$\psi|_{S_i} = a_i - b_i,$$

$$\left.\frac{\partial\psi}{\partial n}\right|_{S_i} = \frac{1}{2\pi R}[-(\alpha + i\beta)a_i + (\alpha - i\beta)b_i], \quad (7)$$

where α and β are the real and imaginary parts of $2\pi kRH_0^{(1)'}(kR)/H_0^{(1)}(kR)$. Using Eqs. (2) and (5) and applying the Green theorem one gets

$$\psi(r) = \sum_i \int_{S_i} \left[G(r,r')\frac{\partial\psi(r')}{\partial n'} - \psi(r')\frac{\partial}{\partial n'}G(r,r')\right] ds', \quad (8)$$

where the sum is over all antennas. In real systems there is an additional contribution from a surface integral along the outer boundary of the billiard because of a partial penetration of the field into the walls. An exact treatment of this effect is beyond the scope of this Letter. Phenomenologically, the walls can be taken into account by introducing an additional channel.

The further evaluation of the integral is easy with help of conditions (7). First one notices that the second term on the right hand side of Eq. (8) is of $O((kR)^2)$. If we restrict ourselves to the situation where R is small compared to the wavelength, this term can be discarded. Taking now for r the value of r_j and using Eq. (7) one gets an equation system for the a_i, b_i which can be written in matrix notation as

$$a - b = G[-(\alpha + i\beta)a + (\alpha - i\beta)b], \quad (9)$$

where the matrix elements of G are given by $G_{ij} = G(r_i, r_j, k)$. Comparing Eqs. (4) and (9) one gets the wanted relation between the S matrix and the Green function,

$$S = \frac{1 + (\alpha + i\beta)G}{1 + (\alpha - i\beta)G}. \quad (10)$$

Equation (10) can still be considerably simplified if at a given k value only one resonance k_n contributes to G. Then the sum (1) reduces to just one term, and the matrix elements of the denominator on the right hand side of Eq. (10) are of the form $M_{ij} = \delta_{ij} + cx_ix_j$. It is easy to verify that the elements of the inverse matrix are given by $M_{ij}^{-1} = \delta_{ij} - bx_ix_j$, where $b = c/(1 + c\sum_k x_k^2)$. Application to Eq. (10) yields

$$S_{ij} = \delta_{ij} + 2(\alpha + i\beta)\hat{G}(r_i, r_j, k), \quad (11)$$

where

$$\hat{G}(r_i, r_j, k) = \sum_n \frac{\psi_n(r_i)\psi_n(r_j)}{k_n^2 - k^2 + \Delta_n - i\Gamma_n} \quad (12)$$

and

$$\Delta_n = \beta\sum_i[\psi_n(r_i)]^2, \quad \Gamma_n = \alpha\sum_i[\psi_n(r_i)]^2. \quad (13)$$

Equations (11) and (12) are the billiard equivalent of the Breit-Wigner formula of nuclear physics [9].

Equation (11) shows that up to a constant factor the modified Green function $\hat{G}(r_i, r_j)$ is obtained directly from the transmission amplitude S_{ij} between the two antennas i and j. $\hat{G}(r_i, r_j)$ differs from the original Green function (1) in two respects. First, the resonances are shifted. This shift was used in Ref. [3] for the

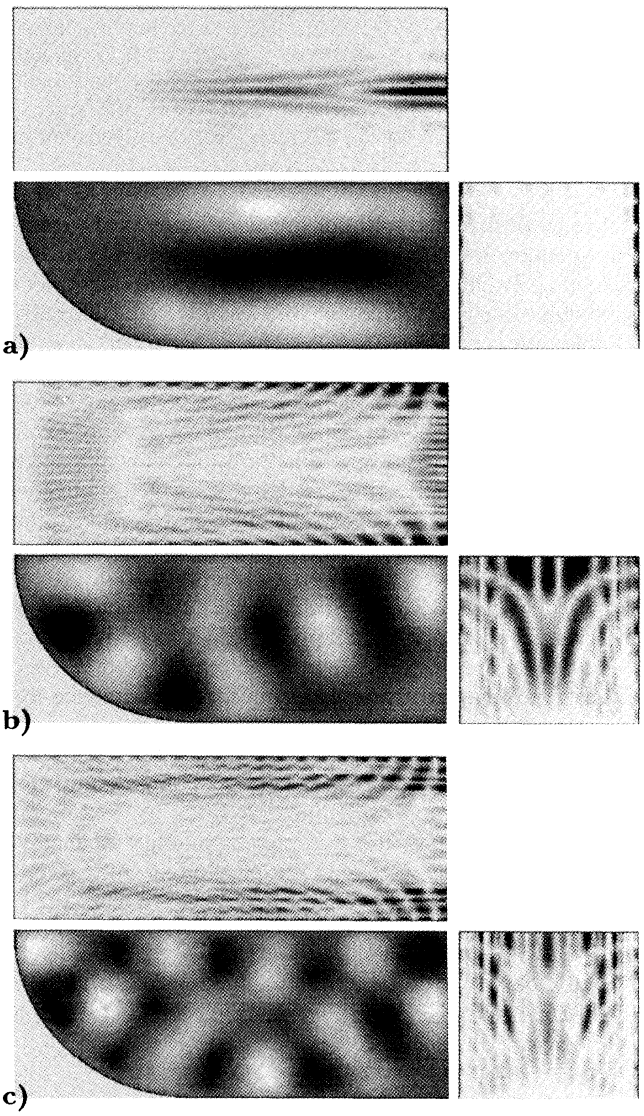

FIG. 1. Experimentally obtained wave functions for three eigenfrequencies 3.228 GHz (a), 4.243 GHz (b), and 5.206 GHz (c) of a quartered stadium (length $a = 180$ mm, width $b = 135$ mm, and height $h = 8$ mm). The upper parts of the figures show the modulus of the corresponding Wigner function taken on the energy surface and for $y = 0$. The abscissa corresponds to x and the ordinate to $p_x/\hbar k_n$, ranging from -1 to $+1$. Classically, this is the cosine of the incidence angle of an incoming classical particle. The right parts show the surfaces of section taken at $x = 0$. Here the ordinate corresponds to y and the abscissa to $p_y/\hbar k_n$. The amplitudes were converted to a gray scale. Black and white correspond to maximal and minimal amplitudes, respectively.

determination of wave functions. It is obvious from Eqs. (13) that the sign of ψ cannot be obtained by this method. Second, the resonances are broadened. Both shift and broadening are unavoidable drawbacks in every experimental determination of the Green function.

The applicability of S-matrix theory to billiards was demonstrated with high precision by Alt *et al.* [10] in a recent experiment using superconducting cavities. The same group studied the situation of closely neighbored resonances [11], where the above derivation becomes invalid. They found a complete agreement between their experimental results and a multilevel expression derived for the case of overlapping resonances.

To test the feasibility of an experimental determination of Green functions, we studied microwave reflection and transmission properties in a stadium-shaped microwave resonator with two antennas. The measuring technique is similar to that applied earlier [4]. The resonator consisted of two parts: a ground plate with an antenna at a fixed position and an upper plate with an excised cavity of the shape of a quartered stadium containing another antenna. The upper plate could be moved with respect to the lower one allowing for a two-dimensional scan of the lower antenna with respect to the billiard. The position of the ground plate antenna was varied in steps of 5 mm in both the x and the y directions leading to a total number of about 1500 data sets. The diameter of the antennas of 0.5 mm was small compared to the wavelength in the whole applied frequency region of 1.6 to 10 GHz. In accordance with Eqs. (13) both width and position of the resonance lines varied by some MHz while changing the antenna position. The complete S matrix was determined as a function of frequency in steps of 1 MHz using a vector network analyzer, model 360B, Wiltron company. A vector network analyzer is indispensable if all S-matrix components are wanted. Strictly speaking, the S matrix of the total system is always measured including cables, connectors, etc. It is possible, however, to calibrate away these unwanted features.

The measurement of S_{12} as a function of r_2 allows the determination of both modulus and sign of the wave functions (in contrast to a S_{11} measurement which gives only the modulus). A variation of r_1 is not necessary for this purpose, if only r_1 is not placed just on a node of the wave function [see Eq. (12)]. There are a number of quantities where both sign and modulus of the wave functions are needed. We mention especially the Wigner function

$$\Psi(p,q) = \frac{1}{(2\pi)^2} \int d^2q' \psi(q - q')\psi(q + q')e^{-2ipq'/\hbar}, \tag{14}$$

which has often been used to study quantum mechanical phase space properties, especially in the semiclassical region (see Ref. [7] for a review). p and q denote the two-dimensional momentum and coordinate vectors, respectively. In the semiclassical region the Wigner function should become concentrated along all periodic orbits contributing to the wave function in question. This is demonstrated in Fig. 1 (though one is here still far from the semiclassical limit). Each of Figs. 1(a)–1(c) consists of three parts. In the lower left the wave function is shown as obtained in the experiment. The upper part shows one surface of section of the corresponding Wigner function calculated from the experimental values. It is taken at the energy surface $p_x^2 + p_y^2 = \hbar^2 k_n^2$ and at $y = 0$ (the upper right corner of the stadium is taken as the origin with x and y axes pointing along the long and the short sides of the billiard, respectively). In the semiclassical limit this is just the Poincaré section for a classical particle taken in the moment of reflection at the upper boundary of the billiard. The right part shows another surface of section of the Wigner function, but now at $x = 0$.

The wave function in Fig. 1(a) represents a standing wave between the long sides of the billiard and is associated with the so-called bouncing ball orbit. In the $y = 0$ surface of section semiclassically one would expect contributions for $p_x = 0$ at all x values in the region of the straight part of the stadium. Indeed the Wigner function shows high amplitudes here. Figure 1(b) is associated with another periodic orbit starting from the upper right corner of the billiard in the southwest direction. Here the $x = 0$ section shows high amplitudes close to the classically expected regions. Figure 1(c) finally shows a wave function with no clear indication of a periodic orbit. The corresponding Wigner function, too, looks rather structureless.

To look for the billiard pulse propagation properties [8], we calculated the electromagnetic propagator from

$$\hat{K}_E(r,r',t) = \frac{1}{2\pi i} \int \hat{G}\left(r,r',\frac{\omega}{c}\right)e^{-i\omega t}d\omega \tag{15}$$

[the quantum mechanical propagator $\hat{K}_Q(r,r',t)$ could be obtained also by replacing $k = \omega/c$ in the argument of the Green function by $k = \sqrt{2m\omega/\hbar}$]. For $t = 0$ $K_E(r,r',t)$ corresponds to a deltalike pulse centered at $r = r'$. Experimentally, however, the integral on the right hand side of Eq. (10) has to be cut off at a certain $\omega_{\max} = 2\pi\nu_{\max}$. With the a $\nu_{\max}$ of 10 GHz this leads to an experimental pulse width of $\Delta r = c/\omega_{\max} = 5$ mm. One may ask why the propagator is not determined directly by sending a microwave pulse through the billiard.

The reason is purely technical: It is much easier to construct a microwave source for continuous waves in the 10 GHz frequency region than to build a pulse generator able to produce pulses of length 10^{-11} s.

Figure 2 shows a series of two-dimensional plots of $K(r,r',t)$ with fixed r for different times. The figure allows an immediate interpretation. Starting at $t = 0$ a circular wave is emitted with a radius R increasing with t according to $R = ct$. Figure 3(a) shows the same situation in a three-dimensional plot. At $t = 1.6 \times 10^{-10}$ s [Fig. 2(b)] the wave reaches the upper bounds of the billiard and is reflected. During reflection the

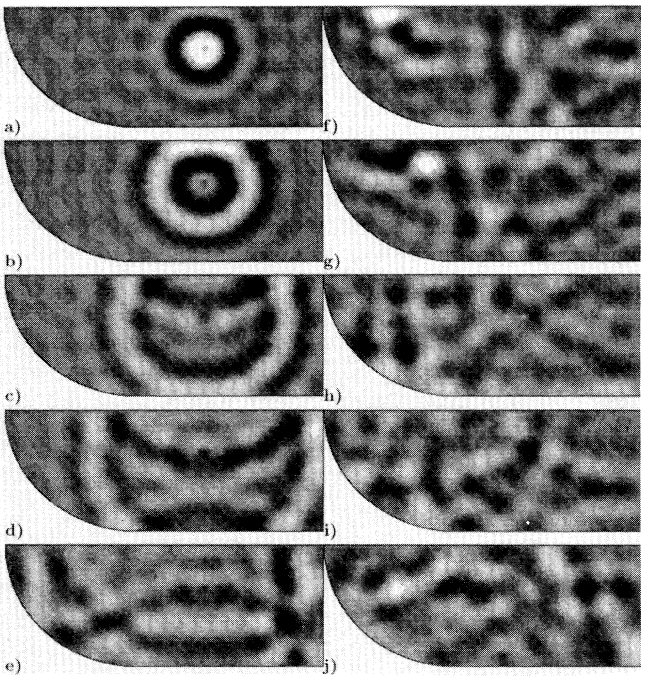

FIG. 2. Two-dimensional plot of the electromagnetic propagator $K_E(r, r', t)$ with fixed r for different times $t/10^{-10}$ s = 0.36 (a), 1.60 (b), 2.90 (c), 3.80 (d), 5.63 (e), 9.01 (f), 10.21 (g), 12.05 (h), 14.18 (i), and 19.09 (j).

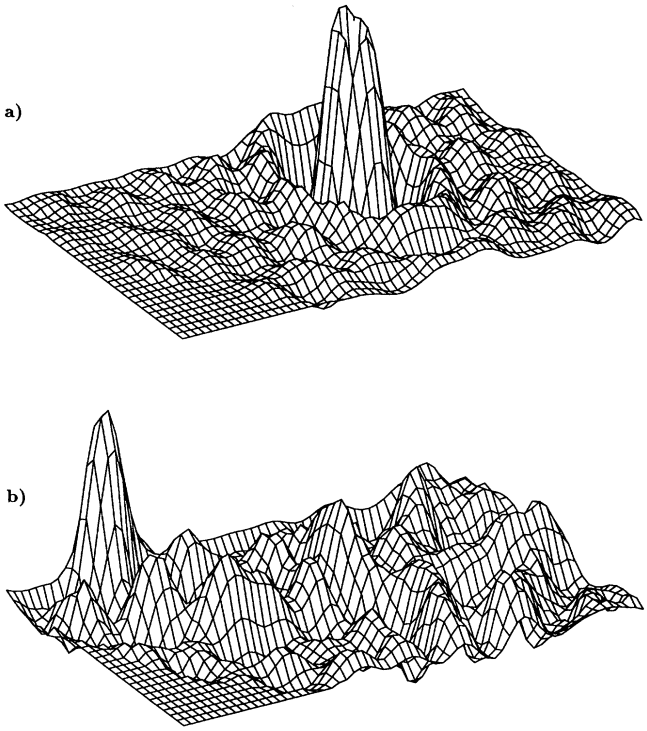

FIG. 3. Three-dimensional map of $K_E(r, r', t)$ for two times $t/10^{-10}$ s = 0.36 (a) and 9.01 (b) corresponding to Figs. 2(a) and 2(f), respectively.

phase of the wave changes by π which is nicely seen in Fig. 2(c). After some more reflections the original pulse is destroyed, and the amplitude is more or less uniformly distributed. But after a considerable elapse of time a sudden reconstruction of the pulse is observed [Figs. 2(f) and 2(g)]. Figure 3(b) shows the situation of Fig. 2(g) three-dimensionally. The cause for this observation is the well-known focusing property of the circle. A similar phenomenon was already found in our earlier reflection measurements in the same system [4]. This is an experimental visualization of the results of Tomsovic and Heller [8]. For times corresponding to the reciprocal distance between neighboring eigenfrequencies (typically several tens of MHz) the propagator becomes reminiscent of the individual eigenstates, which limits the applicability of semiclassical quantum mechanics to times smaller than 10^{-7} s. The maximal times accessible (limited by the experimental line width of about 5 MHz) exceed this value by a factor of 10. Thus the complete transition region between classical and quantum mechanics is within the range of the experiment.

Professor A. Richter, Darmstadt and his group is thanked for stimulating discussions. This work was supported by the Deutsche Forschungsgemeinschaft via the Sonderforschungsbereich "Nichtlineare Dynamik."

[1] H.-J. Stöckmann and J. Stein, Phys. Rev. Lett. **64**, 2215 (1990).
[2] H.-D. Gräf, H. L. Harney, H. Lengeler, C. H. Lewenkopf, C. Rangacharyulu, A. Richter, P. Schardt, and H. A. Weidenmüller, Phys. Rev. Lett. **69**, 1296 (1992).
[3] S. Sridhar, Phys. Rev. Lett. **67**, 785 (1991).
[4] J. Stein and H.-J. Stöckmann, Phys. Rev. Lett. **68**, 2867 (1992).
[5] H. U. Baranger, R. A. Jalabert, and A. D. Stone, Chaos **3**, 665 (1993).
[6] M. V. Berry and K. E. Mount, Rep. Prog. Phys. **35**, 315 (1972).
[7] M. C. Gutzwiller, *Chaos in Classical and Quantum Mechanics* (Springer, New York, 1990).
[8] S. Tomsovic and E. J. Heller, Phys. Rev. Lett. **67**, 664 (1991); Phys. Rev. E **47**, 282 (1993).
[9] J. M. Blatt and V. F. Weisskopf, *Theoretical Nuclear Physics* (John Wiley, New York, 1952).
[10] H. Alt, H.-D. Gräf, H. L. Harney, R. Hofferbert, H. Lengeler, A. Richter, P. Schardt, and H. A. Weidenmüller, Phys. Rev. Lett. **74**, 62 (1995).
[11] H. Alt, P. von Brentano, H.-D. Gräf, R.-D. Herzberg, M. Philipp, A. Richter, and P. Schardt, Nucl. Phys. **A560**, 293 (1993).

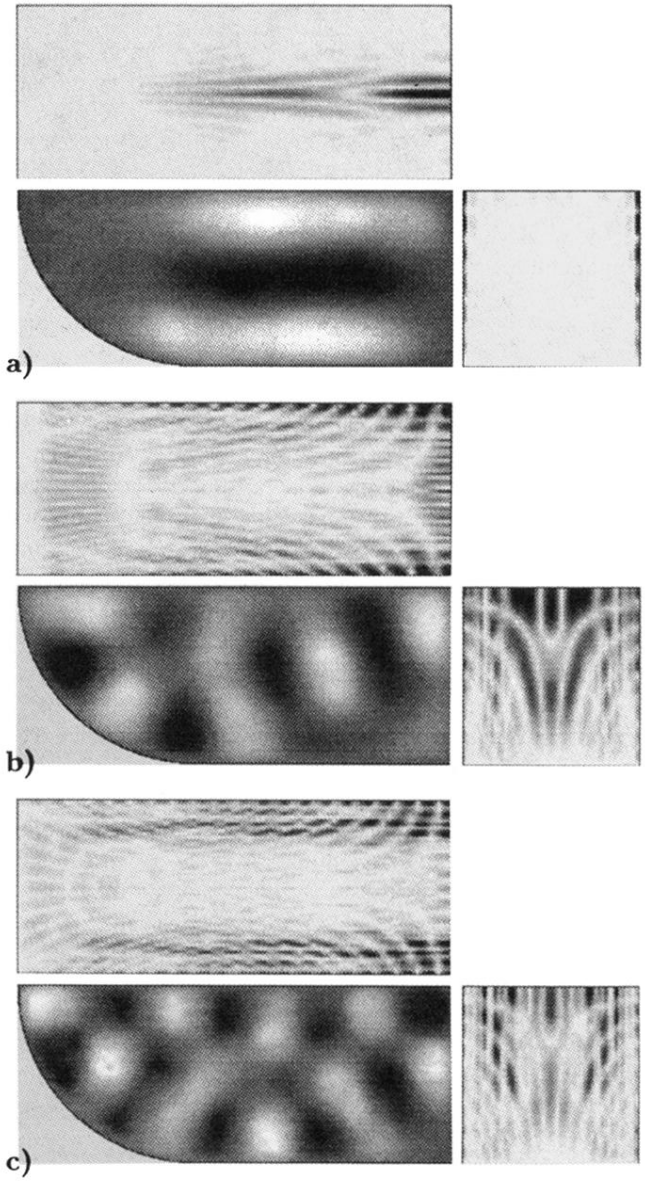

FIG. 1. Experimentally obtained wave functions for three eigenfrequencies 3.228 GHz (a), 4.243 GHz (b), and 5.206 GHz (c) of a quartered stadium (length $a = 180$ mm, width $b = 135$ mm, and height $h = 8$ mm). The upper parts of the figures show the modulus of the corresponding Wigner function taken on the energy surface and for $y = 0$. The abscissa corresponds to x and the ordinate to $p_x/\hbar k_n$, ranging from -1 to $+1$. Classically, this is the cosine of the incidence angle of an incoming classical particle. The right parts show the surfaces of section taken at $x = 0$. Here the ordinate corresponds to y and the abscissa to $p_y/\hbar k_n$. The amplitudes were converted to a gray scale. Black and white correspond to maximal and minimal amplitudes, respectively.

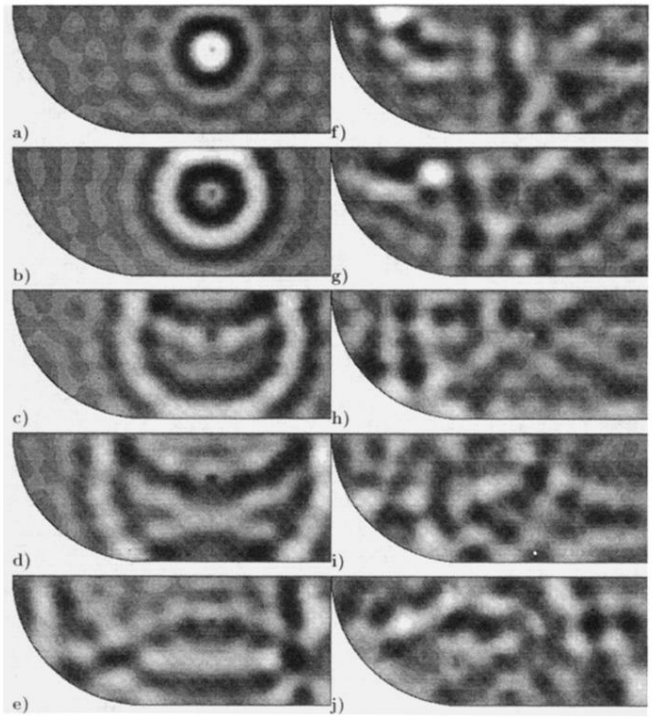

FIG. 2. Two-dimensional plot of the electromagnetic propagator $K_E(r, r', t)$ with fixed r for different times $t/10^{-10}$ s = 0.36 (a), 1.60 (b), 2.90 (c), 3.80 (d), 5.63 (e), 9.01 (f), 10.21 (g), 12.05 (h), 14.18 (i), and 19.09 (j).